Predicting Energies of Small Clusters from the Inhomogeneous Unitary Fermi Gas

J. Carlson[1] and S. Gandolfi[1]

[1] *Theoretical Division, Los Alamos National Laboratory, Los Alamos, NM, 87545*

(Dated: June 16, 2014)

We investigate the inhomogeneous unitary Fermi gas and use the long-wavelength properties to predict the energies of small clusters of unitary fermions trapped in harmonic potentials. The large pairing gap and scale invariance place severe restrictions on the form of the density functional. We determine the relevant universal constants needed to constrain the functional from calculations of the bulk in oscillating external potentials. Comparing with exact Quantum Monte Carlo calculations, we find that the same functional correctly predicts the lack of shell closures for small clusters of fermions trapped in harmonic wells as well as their absolute energies. A rapid convergence to the bulk limit in three dimensions, where the surface to volume ratio is quite large, is demonstrated. The resulting functional can be tested experimentally, and is a key ingredient in predicting possible polarized superfluid phases and the properties of the unitary Fermi gas in optical lattices.

PACS numbers: 71.15.Mb,03.75.Ss,67.85.Lm

arXiv:1406.3591v1 [cond-mat.quant-gas] 13 Jun 2014

The properties of the homogeneous unitary Fermi gas have been the subject of intense experimental and theoretical study over the last decade [1, 2], including studies of the equation of state [3, 4], the spin and density response at high momentum transfer [5], and other properties related to the contact parameter [6]. More recently the inhomogeneous gas is receiving considerable attention, in particular studies of the three- to two-dimensional transition[7], fermions in optical lattices[8–10], and studies of small clusters of cold fermions at unitarity[11, 12]. In this paper we study the inhomogeneous unitary Fermi gas in three dimensions and show that its properties uniquely determine the properties of even very small clusters of trapped fermions.

We show that a relatively simple density functional, obtained by fitting the properties of the unitary Fermi gas in periodic potentials, can accurately reproduce the energy of small clusters of atoms confined in an harmonic trap. This outcome is not only relevant for cold atoms, but is of high interest for nuclear physics, inhomogeneous superconductors, properties of atoms in optical lattices, and in material science (see for example Ref. [9]).

In this work we study the system described by the Hamiltonian:

$$H = \sum_i e_i(q) + g \sum_{k,p,q} a^\dagger_{\uparrow k+q} a^\dagger_{\downarrow p-q} a_{\uparrow k} a_{\downarrow p} + V_{ext}, \quad (1)$$

where the dispersion is either $e_i(q) = q^2/(2m)$, or other improved lattice actions [13], and the potential strength g is tuned to describe infinite scattering length in the two-particle system. The resulting system is the scale invariant Unitary Fermi gas (UFG), characterized by universal constants including the ratio $\xi = E/E_{FG} \approx 0.37$ [3, 13] of the UFG to free Fermi gas energy, that is density independent.

The UFG has many special properties, including a very large ratio of pairing gap to Fermi energy, $\Delta/E_F \approx 0.45(5)$ [14–16], and two universal constants that describe all the long-wavelength excitations [17]. Pairing gaps of the scale of the Fermi energy imply that in the ground state single fermions cannot propagate over long distances, and thus moderate sized clusters of fermions will not exhibit the large shell effects typically found in atoms or nuclei. Large pairing gaps in neutron-rich atomic nuclei have been used to describe shell quenching, or the lack of closed shell gaps in energy versus particle number characteristic of atoms or of nuclei with $N \approx Z$ [18]. In addition, the strong pairing makes these systems behave similarly to Bose gases, where shell effects that are usually evident for Fermions in finite boxes are totally absent for the UFG [19]. The unitary limit provides a clean simple experimental system that can further our understanding of the transition from small systems to the bulk. The energies of a small number of fermions in one dimension have recently been studied experimentally to determine this transition to bulk behavior [12]. In three dimensions one would expect the transition to require much larger systems because of the larger surface to volume ratio.

The two universal constants describing low-energy phonon excitations and the susceptibility to long-wavelength oscillations can be calculated in the bulk. The scale invariance and the large pairing gap place severe restrictions on the density functional of the UFG, i.e. in a gradient expansion all terms must have the same dimension as the free Fermi gas energy density, or one over length to the fifth power, or $\rho^{5/3}$ [17]. The susceptibility as a function of wavelength then completely determines the density functional, and can be used to make unique predictions for small clusters.

In order to calculate the above mentioned properties, we perform both Diffusion Monte Carlo (DMC) and Auxiliary Field Monte Carlo (AFMC) calculations of the inhomogeneous UFG. Both extract the ground state from a Monte Carlo evaluation of $|\Psi_0\rangle = \exp[-H\tau]|\Psi_T\rangle$. The AFMC calculations are exact for a specific lattice size

since they do not suffer from a sign problem [20–22]. The method involves a branching Markov chain Monte Carlo where the states are evolved through a fluctuating auxiliary field. The algorithm is described in [13], the only addition is that we modify the BCS trial state $|\Psi_T\rangle$ multiplying the pairing terms $\phi(r_{ij})$ by a product of two single-particle functions $\Phi(r_1)\Phi(r_2)$. This additional importance sampling lowers the statistical errors considerably for strong external fields. The Markov chain Monte Carlo is implemented as a branching walk, allowing us to extend the calculations to extremely low temperatures with modest variance. We have made calculations on cubic lattices of size L^3, with L=16, 20, 24, and have also used two different dispersion relations $e_i(q)$ (Eq. 1) to eliminate effective-range and other effects from finite lattice spacing.

The DMC calculations provide accurate upper bounds to the ground state energy, but can be performed in the extremely dilute limit compared to the lattice calculations. Other operators can also be easily computed [23]. The DMC calculations use optimized BCS variational wave functions described in [23, 24]. We add long range correlations to the BCS wave function to improve the description of the low energy physics. We first consider the static structure factor $S^0(q) = \langle 0|\rho^\dagger(\mathbf{q})\rho(\mathbf{q})|0\rangle$ with $\rho(\mathbf{q}) = \sum_i \exp[i\mathbf{q}\cdot\mathbf{r}_i]$. The energy and inverse energy weighted sum rules are denoted $S^1(q)$ and $S^{-1}(q)$, respectively. Figure 1 shows $S^0(q)$ obtained from the optimized BCS wave function without (BCS) and with (BCS-J) long-range correlations and the results of our DMC calculations. The trial wave function including long-range Jastrow correlations [25, 26] is:

$$\Psi_{BCS-J} = \prod_{i<j} \exp\left[\gamma \sum_n \frac{\exp(-\lambda|\mathbf{q_n}|)}{|\mathbf{q_n}|} \exp(-i\mathbf{q}\cdot\mathbf{r}_{ij})\right] \Psi_{BCS} \quad (2)$$

where Ψ_{BCS} is the correlated BCS wave function with short-range Jastrow correlations used in previous calculations [23], and γ and λ are variational parameters. The final DMC energies are independent of the choice of these correlations. In Fig. 1 the solid line at low q is the phonon dispersion $S(q) = (q/k_F)\sqrt{3/\xi}/2$, using the convention $\hbar^2/(2m) = 1$. A small deviation from the linear dispersion is apparent at $q/k_F = 0.5$, where we find $S^1(q)/(k_F^2 S^0(q)) = 0.402(5)$.

The static density susceptibility at low q , given by the inverse energy-weighted sum rule $S^{-1}(q)$, determines the long-wavelength behavior of the density functional. The first gradient-squared correction to the local density approximation is unique, we rewrite the density functional obtained in [27] as:

$$\mathcal{E}_2 = \int V_{ext}(r)\rho(r) + \xi\frac{3}{5}(3\pi^2)^{2/3}\rho^{5/3} + c_2\,\nabla\rho^{1/2}\cdot\nabla\rho^{1/2}. \quad (3)$$

The first two terms are the local density approximation (LDA), $\mathcal{E}_2$ depends on only one additional parameter c_2, and remaining terms are of order q^4 or higher. This form makes explicit the connection between the BCS and BEC limits, in this notation $c_2 = 0.111$ in the extended Thomas Fermi model for free fermions, and $c_2 = 0.5$ in the extreme BEC limit. The gradient term is exactly the same as for the Gross-Pitaevskii (GP) equation used to describe Bose-Einstein condensation [28], in this case condensation of pairs. This parameter is important in GP treatments of the dynamics in the unitary gas, including soliton and vortex dynamics [29, 30], and to possible inhomogeneous superfluid (LOFF) phases of the polarized system [31].

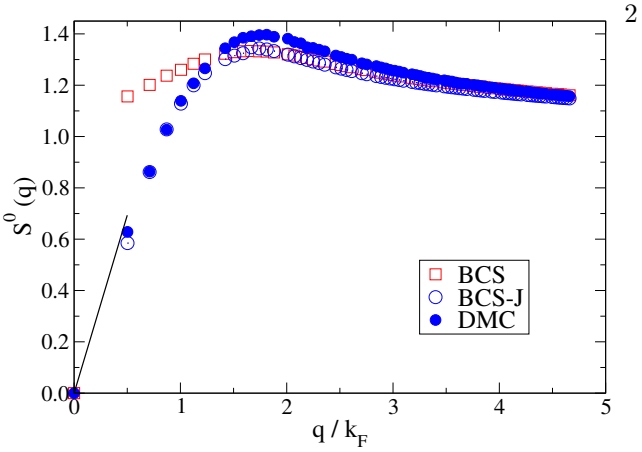

FIG. 1. (Color online) Static structure function for the unitary Fermi gas. The open squares are the BCS result, and the open circles are for the BCS-J variational trial function. The filled circles are the results of the DMC calculation (see text).

To determine the static response at unitarity, we calculate the energy of the system in an external potential $V_{ext} = V_0\ E_F\ \sum_i \cos(\mathbf{q}\cdot\mathbf{r}_i)$, with $E_F \equiv (3\pi^2\rho)^{2/3}$. Initially we choose $V_0 = 0.25$ and $q/k_F = 0.5$ to remain in the low momentum limit and yet have a large enough energy difference with the uniform system to have a statistically meaningful result. From DMC and AFMC results we obtain $c_2 = 0.30(5)$, extracted from a standard bosonic DFT calculation that minimize $\mathcal{E}_2$. The extracted c_2 is larger than that obtained in the ϵ expansion[27], and between the known values in the BCS and BEC regimes. The value $c_2 < 0.5$ implies slower (larger effective mass) dynamics than a simple GP treatment with $c_2 = 0.5$ from two paired fermions. The extracted c_2 and the $S^0(q)$ can be used to fix the two low-energy parameters in the effective field theory[17] and to constrain additional terms in more sophisticated density functionals such at the superfluid local density approximation (SLDA)[19, 32] that include fermionic degrees of freedom and can treat polarized systems.

For larger gradients (larger V_0) higher-order terms become important. We have calculated the energy of 66 particles in periodic boundary conditions for a range of V_0 for $q/k_F = 0.5$ and $q/k_F = 1$, shown in Fig. 2 as lower and upper symbols and bands, respectively. The

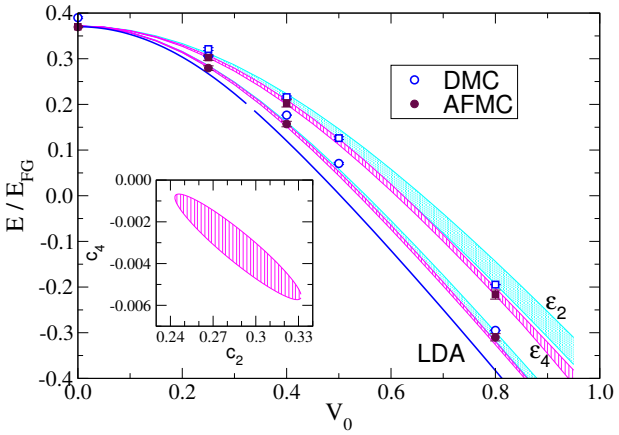

FIG. 2. (Color online) Energy of the unitary Fermi gas in a periodic potential versus strength of the interaction for $q = k_F/2$ (lower curves) and $q = k_F$ (upper curves). Quantum Monte Carlo calculations are shown as symbols. The bands are density functional results for $\mathcal{E}_2$ using $c_2 = 0.30(5)$ and for $\mathcal{E}_4$ with c_2 and c_4 extracted from fits to all the bulk QMC data. See the text for details. The error ellipse obtained for c_2 and c_4 from the fit is shown in the inset.

blue solid line indicates results expected in the local density approximation without gradient terms, entirely determined by ξ. The break in this line represents the point at which the density separates into quasi two-dimensional sheeets. The results of the DMC and AFMC calculations are shown as open and closed symbols respectively.

Using the coefficient c_2 obtained for weak external fields, the QMC calculated energies for $q = 0.5\ k_F$ are well reproduced by this density functional for the whole range of V_0 (lower solid band). This simple density functional is expected to work very well for systems where $|\nabla\rho/(k_F\rho)| << 1$ everywhere. In Fig. 2 it is evident that for the larger $q = k_F$, the $\mathcal{E}_2$ density functional begins to fail, particularly at larger V_0. In this region the higher order gradient corrections are becoming important.

The first correction to the simple gradient density functional $\mathcal{E}_2$ (Eq. 3) is of order q^4 [27]. It is natural to find the energies at higher momenta smaller than those given by $\mathcal{E}_2$, this behavior would be expected based on the typical roton-phonon spectrum [3, 33]. Using the scale invariance of the density functional and a Negele-Vautherin[34] expansion for the density functional in terms of gradients, we add another term

$$\mathcal{E}_4 \;=\; \mathcal{E}_2 \;+\; c_4 \frac{\nabla^2\rho^{1/2}\nabla^2\rho^{1/2}}{\rho^{2/3}}\,, \qquad (4)$$

with the same dimensions as $\mathcal{E}_2$. This additional term is attractive ($c_4 < 0$) since the quasiparticle spectrum lies lower than the simple linear behavior with increasing q.

We perform a simultaneous fit of c_2 and c_4 in $\mathcal{E}_4$ to all the AFMC data to obtain the error ellipse shown in the inset of Fig. 2. For each pair of values c_2 and c_4 a standard DFT calculation of the density is first performed setting $c_4 = 0$, then the energy contribution from the c_4 term in $\mathcal{E}_4$ is calculated perturbatively from this density

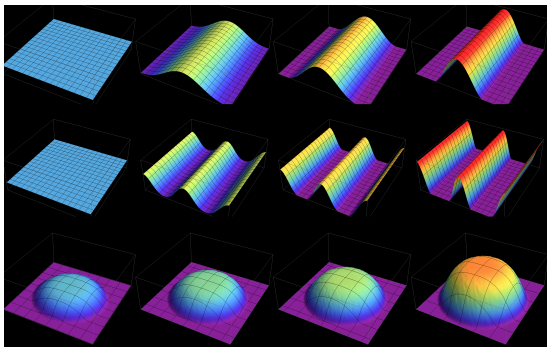

FIG. 3. (Color online) Densities of the unitary Fermi gas in external potentials of frequency $k_F/2$ (upper row) and k_F (middle row) for potential strengths $V_0 = 0$, 0.25, 0.4, and 0.8 from left to right. The lower row shows the predicted density distributions (in the z=0 plane) for systems of 8, 14, 30, and 50 fermions (left to right) in a harmonic trap. Scale invariance requires the energies depend only upon the shape of the density distribution, except for an overall scale of $\rho^{2/3}$.

distribution. Since the q^4 term in $\mathcal{E}_4$ term is attractive, we must evaluate it perturbatively as it is unstable to high-frequency oscillations. Higher-order terms including those associated with the contact would stabilize the system [35].

The extracted error ellipse for these parameters shows a strong correlation since a larger value of c_2 requires a more attractive value of c_4. The solid and vertical hatched regions give the error bands for $\mathcal{E}_2$ and $\mathcal{E}_4$, respectively. The $\mathcal{E}_4$ density functional provides an excellent fit to all the data, with a χ^2 per degree of freedom near one. The width of the bands in the main figure represent varying the coefficients within the quoted uncertainties (the inset ellipse for $\mathcal{E}_4$).

The density functional can then be used to predict the densities of inhomogeneous matter and properties of small numbers of fermions trapped in harmonic wells. Observing the densities in an external field should be an accurate way to measure the coefficients in the density functional. The densities for both inhomogeneous matter and small trapped systems are shown in Fig. 3. The upper two rows illustrate the transition from three towards two dimensional systems with increasing V_0 for external potentials of momenta $k_F/2$ and k_F, and the bottom row shows the densities of small systems trapped in a harmonic potential.

To check the predictions for trapped fermions, we calculate systems of fermions at unitarity in a harmonic trap from 4 to 80 particles (Fig. 4). The square of the ratio of the energy at unitarity to the Thomas Fermi energy for free fermions, $E_{TF} = \omega(3N)^{4/3}/4$, is plotted as a function of the number of particles. This ratio should approach the bulk (LDA) limit as the size of the system increases. The DMC results are shown as blue open circles in the figure, and the AFMC results are shown as diamonds. For $N > 8$, both our DMC and AFMC results are significantly lower than those obtained previ-

ously by Endres, et al.[36], Blume, et al.[37], Chang and Bertsch[38], and by Mukherjee and Alhassid[39]. The AFMC calculations extend to much lower temperature T than previous lattice calculations, and are averaged from $\omega/T \approx 4-10$.

The DMC calculations include a more sophisticated trial wave function than used previously. It includes pairing both in a single-particle orbitals as typically used in atomic nuclei and pairing based upon the local density approximation. The variational wave function for the system in the trap has pairing orbitals with the following form:

$$\Phi(\mathbf{r}_1,\mathbf{r}_2) = \left[\sum_i d_i \phi^{HO}_{n_i}(\alpha_i \mathbf{r}_1)\phi^{HO}_{n_i}(\alpha_i \mathbf{r}_2)\right] e^{-(\gamma_1+\gamma_2)R^2} + \beta[k_F(R)\, r] e^{-\frac{m\omega}{2\hbar}R^2}(1-e^{-\gamma_2 R^2})\,. \quad (5)$$

where n_i are HO quantum numbers of the i-th state, $R = |\mathbf{r}_1+\mathbf{r}_2|/2$, $r = |\mathbf{r}_1-\mathbf{r}_2|$, and the function $k_F(R)$ is the local momentum as a function of the center of mass of the pair: $k_F(R) = \left[\frac{1}{\hbar\xi}(\xi E_F - \omega^2 R^2/2)\right]^{1/2}$, and the function $\beta(r)$ has the same form of Ref. [23]. The variational parameters d_i, α_i and γ_i are optimized, and simulations at different effective ranges to extract the zero-range limit. If we simplify our calculations to the simple trial function used in [37] and [38], we reproduce their higher energies.

The AFMC lattice calculations are exact but subject to finite lattice size errors. Two sets of AFMC calculations are shown, one using the q^2 dispersion relation, the other using the q^2+q^4 dispersion discussed in [13]. The finite-size energy correction for the q^2 dispersion is proportional to the effective range and to the lattice spacing, it is given by:

$$\delta E_{HO}(N)/E_{TF} = -\frac{2048 N^{1/6}\omega^{1/2} S r_e}{525\times 3^{5/6}\pi\xi^{3/4}}. \quad (6)$$

Numerically this yields $\delta E(N)/E_{TF} \approx 0.0388\ \omega^{1/2}N^{1/6}$ for $S = 0.12$, $\xi = 0.37$, and $r_e = 0.337a$ (a is the lattice spacing), the correction is approximately a 2% lowering of the QMC energy. The value of S is extracted from Refs. [13, 40]. Similar corrections have been applied in the bulk, they are significantly smaller than the statistical errors.

Similarly the q^4 propagator requires a correction from pairs of finite momentum, which for small lattice sizes lowers the energy from the continuum behavior. Calculating the energy of a pair with finite momentum yields a correction $\delta E(N)/E = \zeta^2 a^2 (5/6)\langle \mathbf{K}^2\mathbf{k}^2\rangle$, where $\zeta = 0.16137$ is the coefficient of the k^4 term in the propagator, and $\mathbf{k}^2$ and $\mathbf{K}^2$ are the average square momenta of particles and pairs respectively. The former can be estimated from the simulation and the latter from the calculated total energy using the virial theorem. In this case the correction yields an approximately 1% increase

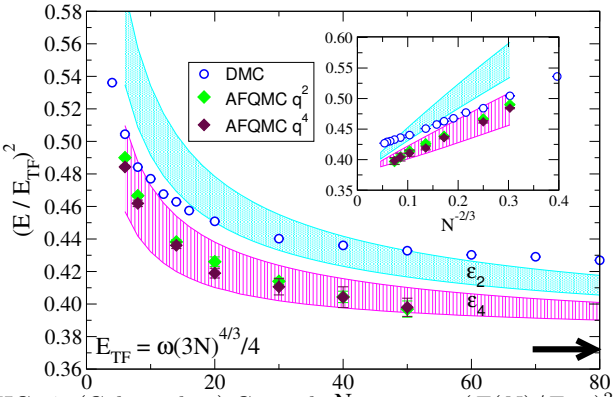

FIG. 4. (Color online) Ground-state energy $(E(N)/E_{TF})^2$ of trapped fermions at unitarity vs. particle number N. Present DMC calculations are shown as open circles, and AFMC calculations as diamonds. Density functional results $\mathcal{E}_2$ and $\mathcal{E}_4$ are shown (see text). The inset shows the extrapolation of the same data to the bulk (large N) limit.

in the energy. This correction is numerically consistent with zero for homogeneous systems as shown by calculations of two species of unequal mass [41, 42]. The two sets of AFMC energies calculated with different dispersions agree within error bars. The corrections for the periodic external potential are much smaller than the error bars since the external interaction confines the system in only one dimension.

The QMC results for small clusters are compared with the predictions from the two different density functionals $\mathcal{E}_2$ and $\mathcal{E}_4$ in Fig. 4. In the local density approximation the ratio of squared energies is a constant ξ for any N, the arrow indicates the bulk value of ξ applicable in the large N limit. The results for $\mathcal{E}_2$ are shown as the upper solid band, and the predictions from $\mathcal{E}_4$ are shown as the lower vertical hatched band. This density functional provides an excellent description of the small trapped systems, the c_4 term is much more important in this case.

As we can see in Fig. 4 our calculations yield no significant shell effects or breaks in the curve of E/E_{TF} curve versus the number of particles. In the BCS limit there would be sharp breaks of the energy with particle number, with closed shells at $N = 2, 8, 20, 40, ...$ for a harmonic oscillator external potential. Shell closures are a natural expectation for many fermionic systems, even those with significant pairing like atomic nuclei or inhomogeneous neutron matter [43]. In the unitary Fermi gas, however, the shell breaks appear quite small, further justifying the density functional in terms of the local density and its gradients. This is to be expected for large systems, where the coherence length is much smaller than the system size. Even for small systems, it would appear that unpaired fermions cannot propagate significantly. This physics has a natural analogue in neutron-rich atomic nuclei, where the pairing gaps play an increasingly important role compared to shell gaps as the number of neutrons increase.

In summary, we find find that the density functional of the Unitary Fermi gas is strongly constrained by the scale invariance of the system and the large pairing gap for sin-

gle particle excitations. A simple density functional with two parameters beyond the LDA can describe the energies of inhomogeneous systems over a very wide range of external potentials. We have extracted the universal values of the density functional coefficients from calculations in a one-dimensional periodic potential, and we find that even very small trapped systems can be successfully predicted by this density functional. These small trapped systems show no evidence of significant shell closures as would be expected for most Fermionic systems. Among other applications, this density functional could be tested by predicting properties of the UFG in optical lattices, and compared with experiments.

We would like to thank Kevin E. Schmidt, Shiwei Zhang and Sebastiano Pilati for stimulating discussions. Computer time was provided by an INCITE allocation and by Los Alamos Institutional Computing. This research used also resources of the National Energy Research Scientific Computing Center, which is supported by the Office of Science of the U.S. Department of Energy under Contract No. DE-AC02-05CH11231. The work of J. Carlson and S. Gandolfi were supported by the Department of Energy Nuclear Physics Office, and by the NUCLEI SciDAC program. The work of S. Gandolfi was also supported by a Los Alamos LDRD early career grant.

[1] S. Giorgini, L. P. Pitaevskii, and S. Stringari, Reviews of Modern Physics **80**, 1215 (2008).
[2] M. Randeria and E. Taylor, ArXiv e-prints (2013), arXiv:1306.5785 [cond-mat.quant-gas].
[3] M. J. H. Ku, A. T. Sommer, L. W. Cheuk, and M. W. Zwierlein, Science **335**, 563 (2012).
[4] N. Navon, S. Nascimbène, F. Chevy, and C. Salomon, Science **328**, 729 (2010).
[5] S. Hoinka, M. Lingham, M. Delehaye, and C. J. Vale, Phys. Rev. Lett. **109**, 050403 (2012).
[6] S. Hoinka, M. Lingham, K. Fenech, H. Hu, C. J. Vale, J. E. Drut, and S. Gandolfi, Phys. Rev. Lett. **110**, 055305 (2013).
[7] A. T. Sommer, L. W. Cheuk, M. J. H. Ku, W. S. Bakr, and M. W. Zwierlein, Phys. Rev. Lett. **108**, 045302 (2012).
[8] I. Bloch, J. Dalibard, and W. Zwerger, Rev. Mod. Phys. **80**, 885 (2008).
[9] P. N. Ma, S. Pilati, M. Troyer, and X. Dai, Nat. Phys. **8**, 601 (2012).
[10] S. Pilati, I. Zintchenko, and M. Troyer, Phys. Rev. Lett. **112**, 015301 (2014).
[11] G. Zürn, A. N. Wenz, S. Murmann, T. Lompe, and S. Jochim, (2013), arXiv:1307.5153 [cond-mat.quant-gas].
[12] A. N. Wenz, G. Zürn, S. Murmann, I. Brouzos, T. Lompe, and S. Jochim, (2013), arXiv:1307.3443 [cond-mat.quant-gas].
[13] J. Carlson, S. Gandolfi, K. E. Schmidt, and S. Zhang, Phys. Rev. A **84**, 061602 (2011).
[14] J. Carlson and S. Reddy, Phys. Rev. Lett. **95**, 060401 (2005).
[15] J. Carlson and S. Reddy, Phys. Rev. Lett. **100**, 150403 (2008).
[16] A. Schirotzek, Y.-I. Shin, C. H. Schunck, and W. Ketterle, Phys. Rev. Lett. **101**, 140403 (2008).
[17] D. T. Son and M. Wingate, Annals of Physics **321**, 197 (2006).
[18] J. Dobaczewski, I. Hamamoto, W. Nazarewicz, and J. A. Sheikh, Phys. Rev. Lett. **72**, 981 (1994).
[19] M. McNeil Forbes, (2012), arXiv:1211.3779 [cond-mat.quant-gas].
[20] J.-W. Chen and D. B. Kaplan, Phys. Rev. Lett. **92**, 257002 (2004).
[21] D. Lee and T. Schäfer, Phys. Rev. C **72**, 024006 (2005).
[22] A. Bulgac, J. E. Drut, and P. Magierski, Phys. Rev. Lett. **96**, 090404 (2006).
[23] S. Gandolfi, K. E. Schmidt, and J. Carlson, Phys. Rev. A **83**, 041601 (2011).
[24] S. Sorella, Phys. Rev. B **64**, 024512 (2001).
[25] L. Reatto and G. V. Chester, Phys. Rev. **155**, 88 (1967).
[26] E. Vitali, P. Arrighetti, M. Rossi, and D. Galli, Molecular Physics **109**, 2855 (2011).
[27] G. Rupak and T. Schäfer, Nuclear Physics A **816**, 52 (2009), arXiv:0804.2678 [nucl-th].
[28] F. Dalfovo, S. Giorgini, L. P. Pitaevskii, and S. Stringari, Rev. Mod. Phys. **71**, 463 (1999).
[29] T. Yefsah, A. T. Sommer, M. J. H. Ku, L. W. Cheuk, W. Ji, W. S. Bakr, and M. W. Zwierlein, Nature (London) **499**, 426 (2013).
[30] A. Bulgac, M. M. Forbes, M. M. Kelley, K. J. Roche, and G. Wlazłowski, Phys. Rev. Lett. **112**, 025301 (2014).
[31] A. Bulgac and M. M. Forbes, Phys. Rev. Lett. **101**, 215301 (2008).
[32] A. Bulgac, Phys. Rev. A **76**, 040502 (2007).
[33] E. Taylor, H. Hu, X.-J. Liu, L. P. Pitaevskii, A. Griffin, and S. Stringari, Phys. Rev. A **80**, 053601 (2009).
[34] J. W. Negele and D. Vautherin, Phys. Rev. C **5**, 1472 (1972).
[35] D. T. Son and E. G. Thompson, Phys. Rev. A **81**, 063634 (2010).
[36] M. G. Endres, D. B. Kaplan, J.-W. Lee, and A. N. Nicholson, Phys. Rev. A **84**, 043644 (2011).
[37] D. Blume, J. von Stecher, and C. H. Greene, Phys. Rev. Lett. **99**, 233201 (2007).
[38] S. Y. Chang and G. F. Bertsch, Phys. Rev. A **76**, 021603 (2007).
[39] A. Mukherjee and Y. Alhassid, Phys. Rev. A **88**, 053622 (2013).
[40] M. M. Forbes, S. Gandolfi, and A. Gezerlis, Phys. Rev. A **86**, 053603 (2012).
[41] J. Carlson, S. Gandolfi, and A. Gezerlis, Progress of Theoretical and Experimental Physics **2012**, 01A209 (2012).
[42] A. Gezerlis, S. Gandolfi, K. E. Schmidt, and J. Carlson, Phys. Rev. Lett. **103**, 060403 (2009).
[43] S. Gandolfi, J. Carlson, and S. C. Pieper, Phys. Rev. Lett. **106**, 012501 (2011).